A Climatology of Nocturnal Warming Events Associated with Cold-Frontal Passages in Oklahoma

ANITA NALLAPAREDDY

School of Meteorology, University of Oklahoma, Norman, Oklahoma

ALAN SHAPIRO

School of Meteorology, and Center for Analysis and Prediction of Storms, University of Oklahoma, Norman, Oklahoma

JONATHAN J. GOURLEY

NOAA/National Severe Storms Laboratory, Norman, Oklahoma

(Manuscript received 18 January 2011, in final form 3 May 2011)

ABSTRACT

A sudden increase in temperature during the nighttime hours accompanies the passages of some cold fronts. In some cold front–associated warming events, the temperature can rise by as much as 10°C and can last from a few minutes to several hours. Previous studies suggest that these events are due to the downward transport of warmer air by the strong and gusty winds associated with the cold-frontal passages. In this study, a climatology of nocturnal warming events associated with cold fronts was created using 6 yr of Oklahoma Mesonetwork (Mesonet) data from 2003 to 2008. Nocturnal warming events associated with cold-frontal passages occurred surprisingly frequently across Oklahoma. Of the cold fronts observed in this study, 91.5% produced at least one warming event at an Oklahoma Mesonet station. The winter months accounted for the most events (37.9%), and the summer months accounted for the fewest (3.8%). When normalized by the monthly number of cold-frontal passages, the winter months still had the most number of warming events. The number of warming events increased rapidly from 2300 to 0200 UTC; thereafter, the number of events gradually decreased. A spatial analysis revealed that the frequency of warming events decreased markedly from west to east across the state. In contrast, the average magnitude of the warming increased from west to east. In contrast to control periods (associated with cold-frontal passages without nocturnal warming events), warming events were associated with weaker initial winds and stronger initial temperature inversions. Moreover, the nocturnal temperature inversion weakened more during warming events than during control periods and the surface wind speeds increased more during warming events than during control periods. These results are consistent with previous studies that suggest the warming events are due to the ''mixing out'' of the nocturnal temperature inversion.

1. Introduction

An intriguing feature of some cold fronts is the sudden, temporary increase in temperature during the nighttime hours that can sometimes accompany their passages. Such nocturnal warming events have been documented in central Australia (Smith et al. 1995; Reeder et al. 2000; Beringer and Tapper 2000), Oklahoma (Sanders and Kessler 1999; Doswell and Haugland 2007; Shapiro et al. 2009), and Mississippi (White 2009). These studies have reported on the conditions prior to the warming episodes, change in conditions as the surface temperature increases, impacts on the magnitude of warming due to local topographic and vegetation features, spatial organization of warming episodes, and characteristics of the associated synoptic-scale cold fronts. These case studies of nocturnal warming episodes associated with cold-frontal passages have led to explanatory physical models of their evolution. The study presented herein complements these studies by providing, for the first time, a climatological description of the episodes' occurrences.

Corresponding author address: Alan Shapiro, University of Oklahoma, 120 David L. Boren Blvd., Room 5900, Norman, OK 73072.
E-mail: ashapiro@ou.edu

DOI: 10.1175/JAMC-D-11-020.1

Specifically, we use a 6-yr dataset of Oklahoma Mesonetwork (hereinafter shortened to Mesonet) observations to address the following questions: How often do nocturnal warming events occur with a given cold-frontal passage over Oklahoma? What is the typical magnitude of the surface temperature rise? What are the hourly, seasonal, and spatial distributions of the warming episodes? Are the conditions prior to and during warming episodes similar to those reported in other studies?

The above studies noted calm–light winds prior to the arrival of cold fronts that led to nocturnal warming. In addition, Sanders and Kessler (1999) and Shapiro et al. (2009) observed that skies were predominantly clear. White (2009) noted that fog was present at the surface but, above the fog, the sky was clear prior to the cold front's arrival. Clear skies and light winds promote enhanced radiational cooling at the surface (Wallace and Hobbs 2006). Consequently, the surface cools at a faster rate than the air aloft and a shallow temperature inversion above the surface can develop. Doswell and Haugland (2007) and White (2009) confirmed from soundings that a strong temperature inversion was present near the surface prior to the cold front's arrival. As the warming events commenced, the wind speeds increased, sometimes dramatically, suggesting that relatively warmer air from aloft was being mixed down toward the surface. The magnitude of warming was observed to range from 1°C (Smith et al. 1995) to as much as 8°C (Doswell and Haugland 2007).

Clarke et al. (1981) provided some clues as to the initiation of mixing in a study of morning glory development in Australia's Gulf of Carpentaria. They suggested that waves propagating on an inversion occasionally mixed the relatively warmer air from aloft down to the surface to produce multiple but short-lived warming events. In a similar study, Smith et al. (1995) observed small (~1°C) rises in surface temperature as waves propagated ahead of a cold front and mixed out the nocturnal inversion. White (2009) described three moderately strong nocturnal warming events that occurred within the cold air mass behind a cold front that had passed through the previous night. White suggested that the warming may have been associated with the propagation of waves on the inversion surface.

The occurrence and magnitude of warming can be impacted by local gradients in elevation and vegetation and can lead to considerable variability in the cooling that occurs prior to the cold front's arrival. A few studies reported that larger magnitudes of warming were associated with larger magnitudes of cooling that occurred beforehand. For instance, Sanders and Kessler (1999) examined several cases of rapid warming and cooling from a thermograph at the Great Plains Apiaries (GPA) station in central Oklahoma. The GPA station is situated in a shallow valley approximately 43 km south-southeast of a station at the Will Rogers International Airport (OKC) that was located at the top of a small butte. Prior to the cold-frontal passage, the temperature at GPA was 6°C colder than at OKC. When the cold front passed through, GPA warmed by 7°C while temperatures only fluctuated by roughly 0.5°–1.5°C at OKC.

Additionally, Doswell and Haugland (2007) examined conditions at the Norman Mesonet station in central Oklahoma during a warming episode associated with a nocturnal cold-frontal passage. Conditions at Norman were compared with those from two other stations in central Oklahoma: one in open grassland (Washington) and the other in a forested creek valley (station CR18 in the Crosstimber Micronet; Haugland 2006). The Norman station is in open grassland but is not as exposed as the Washington station (Doswell and Haugland 2007). Shortly before the frontal passage, the temperature at CR18 dropped by 10°C more than that at the Norman and Washington stations. When the cold front passed through, CR18 warmed by 8.3°C while Washington warmed by only ~2°C. The Norman station warmed by ~6°C. Thus, the station that cooled the most prior to the frontal passage also warmed the most during the frontal passage.

Shapiro et al. (2009) observed a similar phenomenon at a much finer scale using 28 temperature and humidity sensors spaced approximately 30 m apart at the Lake Thunderbird Micronet in central Oklahoma. This micronet is situated on land with variable elevation and vegetation. Its northern edge is near a hilltop approximately 22 m higher in elevation than the forested southern end, which borders Lake Thunderbird. Prior to the cold-frontal passages, stations within the forest at the lower elevations cooled the most. As a result, there was a peak temperature difference of 4°C between the stations at the bottom of the hill and those at the top. As the cold front passed through, stations at the bottom of the hill warmed by as much as ~7°C while stations at the top warmed by only ~3°C.

The latter three studies (Sanders and Kessler 1999; Doswell and Haugland 2007; Shapiro et al. 2009) suggested that sheltering a station from wind, before the passage of a cold front, was an important factor to the occurrence and magnitude of warming. Specifically, the shielding promoted enhanced surface cooling in advance of the mixing that impacted the magnitude of the observed temperature increases. By the end of the warming event, the variations in surface temperature were greatly reduced. White (2009), however, has offered a slightly different perspective on sudden nocturnal warming events captured by the Mississippi Mesonet. Nocturnal

FIG. 1. Locations of the Oklahoma Mesonet stations in commission from 1 Jan 2003 to 31 Dec 2008. Solid lines demarcate Oklahoma's nine NCDC climate divisions.

warming events were partitioned into four categories, one of which contained cold front–associated warming events (warming caused by synoptic or mesoscale boundaries). Looking at all nocturnal warming events (i.e., not restricted to those produced by cold fronts), White suggested that sheltering from wind before warming may not be as important as the intensity of the wind gusts during the warming episode.

Though there can be significant interstation variability with warming events due to topographic and vegetation gradients, warming can be widespread along a cold front. In the case described by Shapiro et al. (2009), warming was observed at 10 surface weather observation stations whose locations ranged from southwest Oklahoma to southeast Missouri. Reeder et al. (2000) also observed a narrow strip of warming along a cold front as it passed through central Australia. Doswell and Haugland (2007) observed a wide swath of mixing-induced warming that spanned ~10 counties near central Oklahoma.

A climatological study of warming events can be used to gauge the potential impacts of warming events and to inform process studies involving, for example, the numerical modeling of cold-frontal mixing–warming events. If a warming event was misforecast, it could result in an underestimated low temperature or an overestimated duration of a cold temperature category. Conceivably, a warming event could lead to the melting of snow and ice, with the subsequent refreezing causing a road hazard. Misforecasting warming events could have ramifications for the energy management, transportation, and agriculture sectors.

The present study provides a climatology of nocturnal warming events associated with cold fronts traversing the state of Oklahoma from 1 January 2003 to 31 December 2008. The organization of this paper is as follows: a description of the primary data sources and the methodology of detecting warming events associated with cold-frontal passages, identifying control periods, and objectively analyzing the warming events' spatial patterns is provided in section 2. The magnitude, temporal characteristics, spatial patterns, and conditions prior to and immediately following warming episodes are presented in section 3. A summary and ideas for possible future research follow in section 4.

2. Datasets and methodology

a. Oklahoma Mesonet data

Data collected by the Oklahoma Mesonetwork were the primary data source used in this study. Commissioned in 1994, the Mesonet is a network of automated weather stations deployed over the state of Oklahoma (Fig. 1). With spacing between stations of approximately 30 km, there is at least one Mesonet station in each county (Fiebrich and Crawford 2001). This study spans from 1 January 2003 to 31 December 2008. Our analysis is based on data from 111 of these stations—the stations that were in commission for our entire study period. The following Mesonet data variables were considered in this study: air temperature at 1.5 and 9 m above ground level (AGL), relative humidity at 1.5 m AGL, wind speed and direction at 10 m AGL, precipitation, and solar radiation. All variables are available at a 5-min reporting period.

The accuracy and response times of the sensors, the quality control procedures, and other details concerning

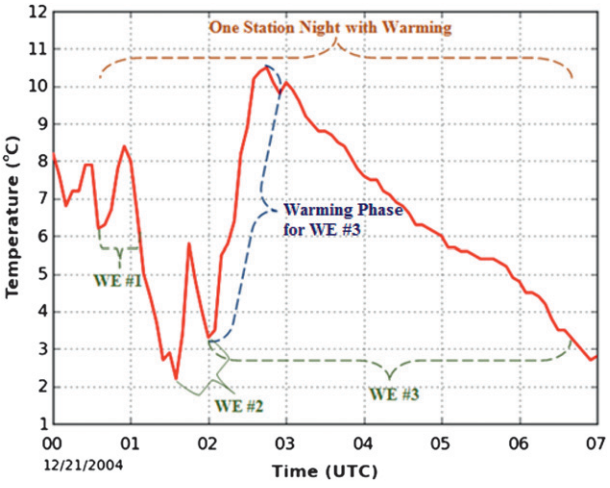

FIG. 2. Temperature at 1.5 m AGL at the Cheyenne Mesonet station. The WE indicates a warming event.

Mesonet data can be found in Shafer et al. (1993, 2000), Brock et al. (1995), and McPherson et al. (2007, 2011). Because previous studies had documented sudden temperature increases up to 8°C during nocturnal cold-frontal passages, we reviewed the Mesonet's quality control procedures to ensure that such events would not be erroneously flagged as bad data and subsequently removed from the dataset. Mesonet observations are checked via five automated tests: range, persistence, spatial, like-instrument, and step tests. The range test flags observations that do not fall within an appropriate range specific to a certain measured variable. Observations of air temperature at 1.5 m, for example, cannot fall outside the range from −30° to 50°C. The persistence test flags observations that vary too little during a calendar day based on the calculated standard deviation of the observations relative to established thresholds. The spatial test utilizes Barnes objective analysis to flag observations that vary too much (exceed a fraction of the standard deviation of the observations within a prescribed radius of influence) between neighboring observations. This test has been tuned so as to tolerate the greater spatial variability found along frontal boundaries (Shafer et al. 2000). The like-instrument test compares 1.5- and 9-m air temperatures and flags differences greater than 10°C. The step test flags unrealistic jumps in data from one observation time to the next. For our purposes, the step test on temperature is particularly relevant: air temperature at 1.5 m cannot change by 10°C or more from one 5-min observation to the next. This test puts an upper bound on the rate of temperature increase that could be documented in our study.

b. Detection of cold-frontal passages

The first step in detecting cold fronts that had associated warming events was the identification of each cold front that passed through Oklahoma during the study period. Automating the detection of synoptic-scale cold-frontal passages was considered, but it was determined that manual identification yielded a more reliable dataset on the timing of cold-frontal passages. First, hand-analyzed surface maps, provided by the National Centers for Environmental Prediction (NCEP) (Colorado State University 2009), were used to manually identify days on which cold fronts passed through Oklahoma. If these maps were unavailable for a particular day, digital surface maps provided by NCEP (2009) and Unisys Weather (2009) were used instead. These latter two sources of data were used to identify approximately 12% of the 365 total cold fronts identified and analyzed in this study.

Next, each Mesonet station was grouped into National Climatic Data Center (NCDC) climate divisions (NCDC 2009). For each of the nine Oklahoma climate divisions shown in Fig. 1, the dates and approximate times of the first appearance of each cold front were recorded. Three stations that were deemed likely to be among the first impacted by a cold front in each division were selected for further analysis. One station was chosen in the westernmost portion of a climate division so that easterly-progressing cold fronts would be detected at the earliest possible time. A second station was selected to be either in the farthest northwest corner of the division or the northernmost location so as to detect the more typical cold fronts that enter the state from a northerly or northwesterly direction. The third station was in the northeasternmost portion of the climate division to aid in the early detection of "back door" cold fronts.

The meteograms showing daily time series of 1.5-m air temperature and dewpoint, 10-m wind direction, wind speed and gusts, and surface barometric pressure at the three selected stations were examined for each climate division to manually approximate the time of the frontal passage. Wind shifts that consisted of a sudden shift from any direction toward a northerly wind direction (between west-northwest and east-northeast) were considered to be strong indicators of cold-frontal passages. If the winds were already coming from a northerly direction before a cold-frontal passage, perhaps due to a prefrontal trough or the passage of a previous cold front, significant increases in wind speed or drops in temperature were used as indicators. In cases in which there was no apparent wind shift, increase in wind speed, or drop in temperature in any of the three meteograms, the previously mentioned surface analyses

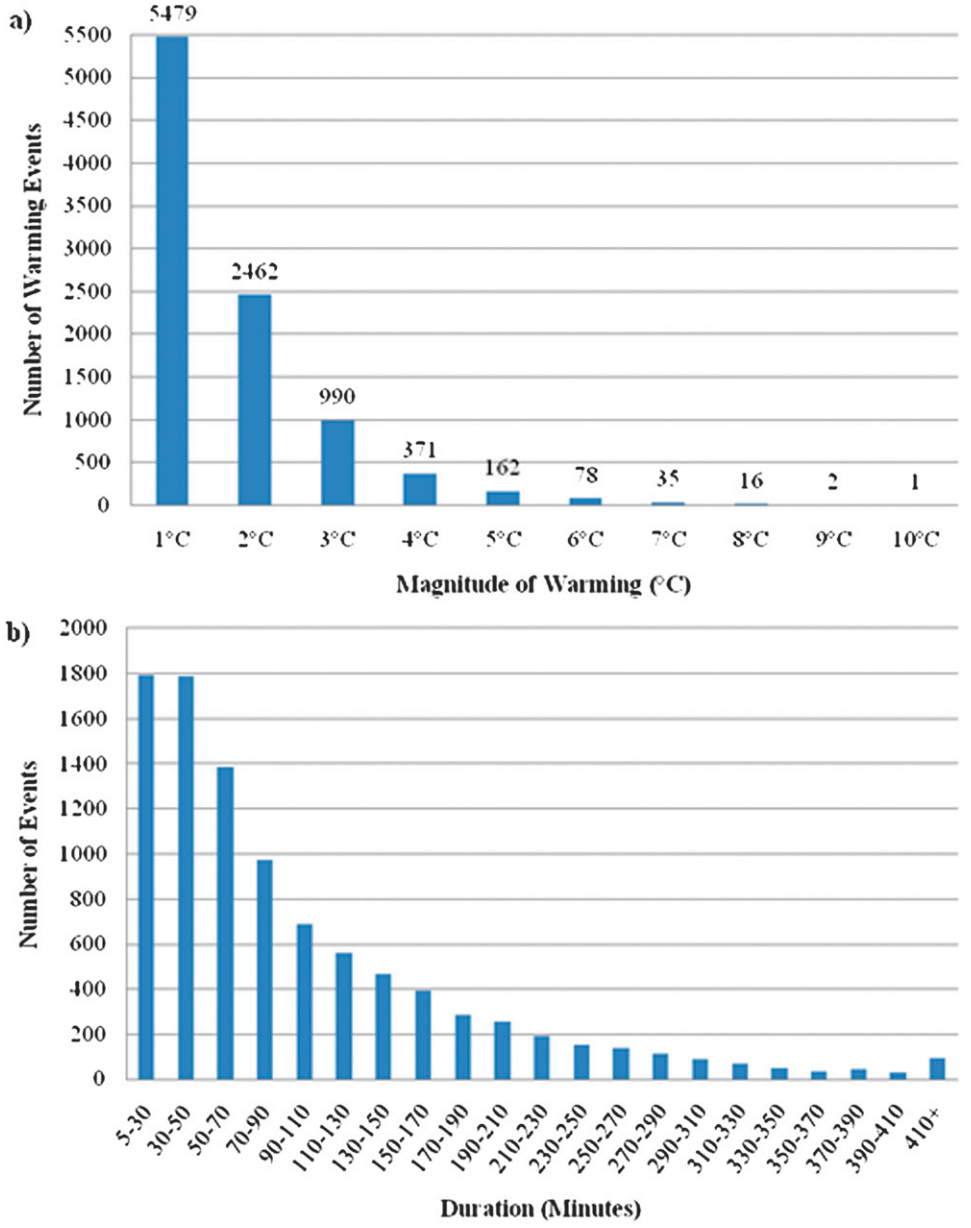

FIG. 3. Total number of warming events from 1 Jan 2003 to 31 Dec 2008 categorized by (a) magnitude and (b) duration.

were used to approximate the time of passage of the cold front.

c. *Automated detection of nocturnal warming events associated with cold fronts*

An automated process was applied to all of the Mesonet data during the study period to find all nocturnal warming events associated with the cold-frontal passages identified by the procedure in section 2b. For brevity we will henceforth refer to these events simply as "warming events." As in the working definitions of other meteorological phenomena—for example, cold fronts, low-level jets, and tornadoes—our definition of a warming event contains a number of arbitrary and subjective elements. We now introduce our particular definition of a warming event.

A warming event commenced with a rise in 1.5-m temperature and ended when the 1.5-m temperature returned to its initial prewarming value, a new warming event began, or solar radiation exceeded 5 W m^{-2} (to ensure a focus on nocturnal warming events). We

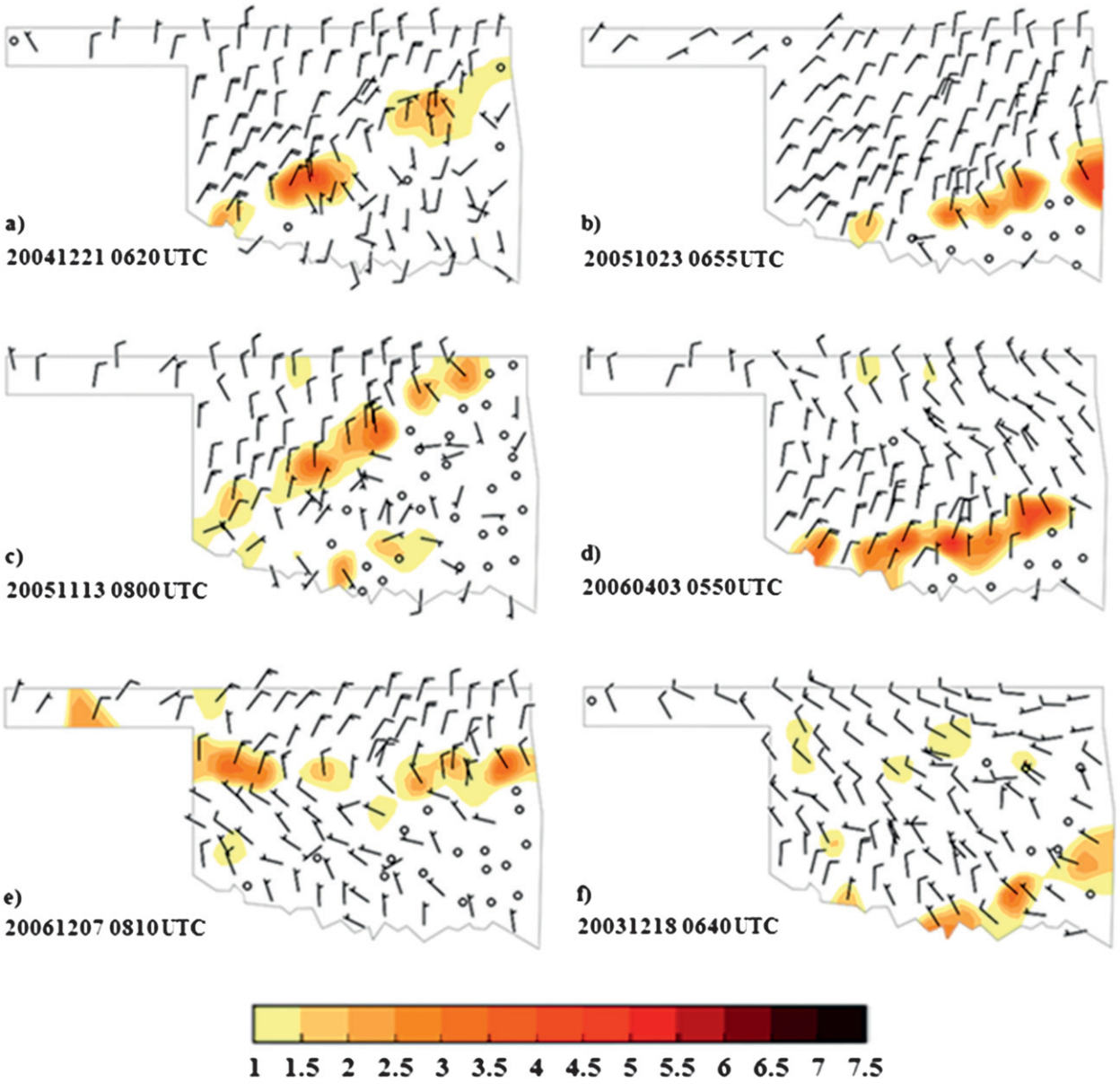

FIG. 4. Barnes analysis depicting maximum 10-min temperature increase (°C) at (a) 0550–0620 UTC 21 Dec 2004, (b) 0625–0655 UTC 23 Oct 2005, (c) 0730–0800 UTC 13 Nov 2005, (d) 0520–0550 UTC 3 Apr 2006, (e) 0740–0810 UTC 7 Dec 2006, and (f) 0610–0640 UTC 18 Dec 2003. Wind barbs are in meters per second with one full barb = 5 m s^{-1}. Wind barbs are valid at the time stamped on the figure.

define the warming phase of a warming event as the time period over which the temperature continues to increase. These terminologies are illustrated in Fig. 2. In addition, a warming-phase detection must satisfy all of the following criteria:

- The warming phase began within 24 h of a recorded cold-frontal passage.
- The wind direction was between 67.5° west of north (west northwest) and 67.5° east of north (east northeast) and persisted for at least 1 h after the end of the warming phase.
- Solar radiation was less than or equal to 5 W m^{-2}.
- The maximum wind speed was at least 2 m s^{-1} during the warming phase.
- No precipitation occurred in the period extending from 3 h before the warming to 3 h after the cessation of warming.
- The temperature increased by at least 1°C during a 10-min interval.

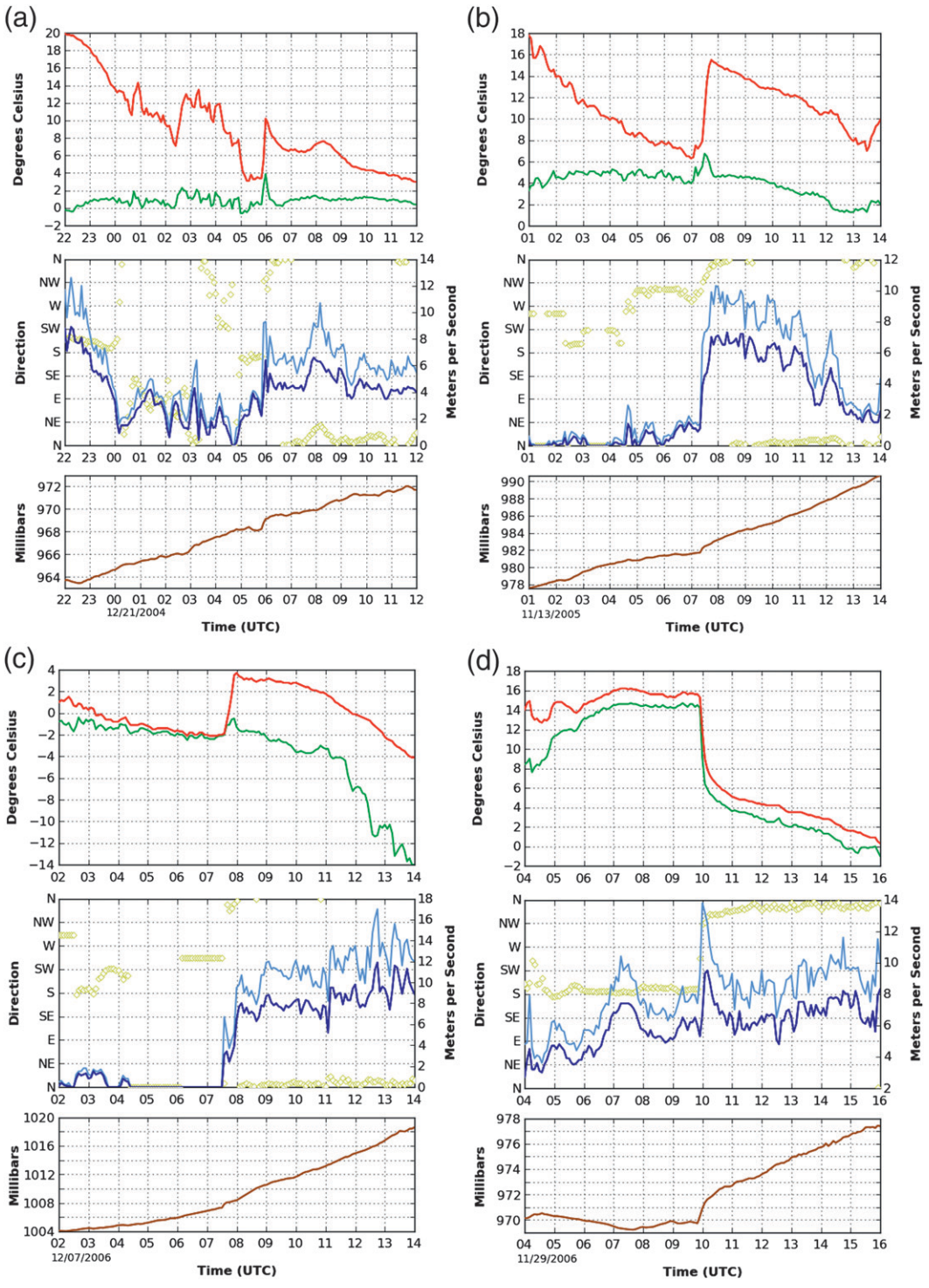

FIG. 5. (a) Surface data from the Chickasha Mesonet station on 20–21 Dec 2004 showing (top to bottom) 1.5-m temperature (red) and dewpoint (green), 10-m wind direction (yellow) on the primary axis and wind speed (dark blue) and gusts (light blue) on the secondary axis, and atmospheric pressure (brown). Sunset occurred at ~2300 UTC 21 Dec. (b) As in (a), but for the Stillwater Mesonet station on 13 Nov 2005. Sunset occurred at ~0000 UTC. (c) As in (a), but for the Bixby Mesonet station on 7 Dec 2006. Sunset occurred at ~0000 UTC. (d) As in (a), but for the Kingfisher Mesonet station on 29 Nov 2006. Sunset occurred at ~2300 UTC 28 Nov 2006.

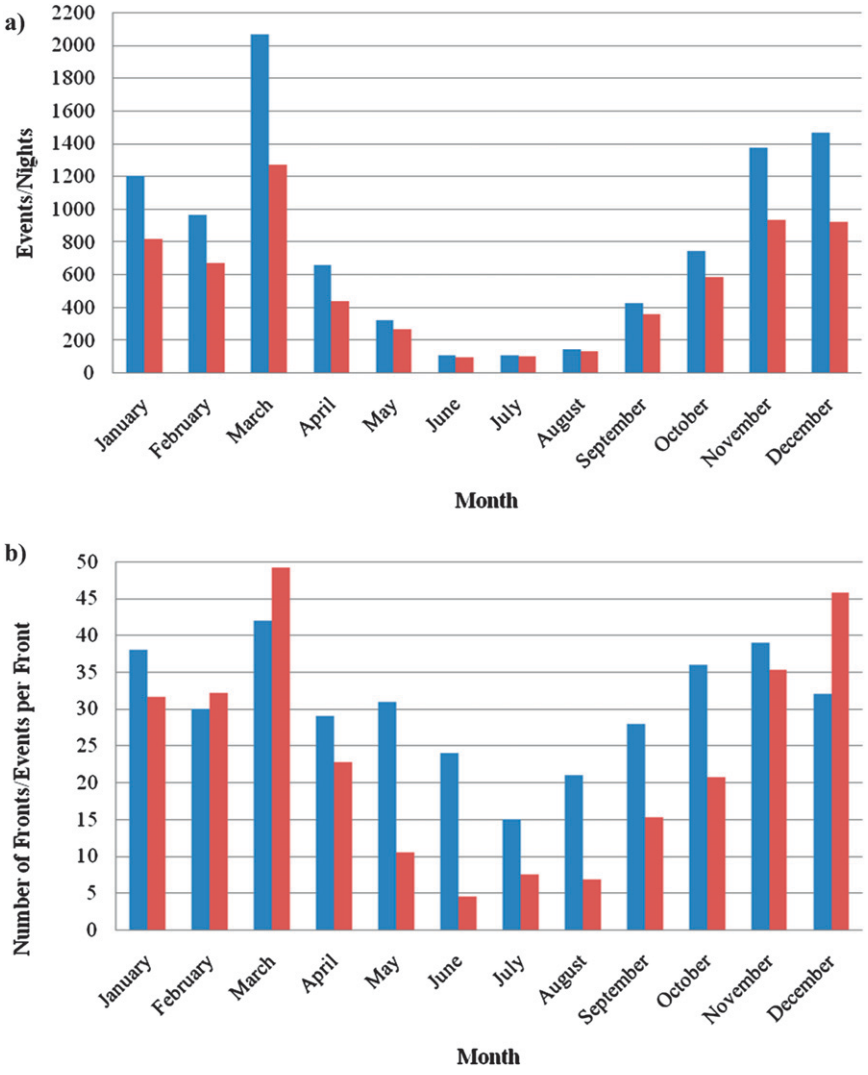

FIG. 6. (a) Total number of warming events (blue) and SNWW (red) categorized by month. (b) Total number of cold-frontal passages (blue) through Oklahoma and total number of events divided by the number of fronts (red) for each month.

- The duration of increasing (or constant) temperatures was limited to 60 min.

The first two criteria were established to ensure that each warming phase was associated with a cold-frontal passage. The range of wind directions considered is typical of observed cold-frontal passages in Oklahoma. The third criterion ensured that the events were nocturnal. A minimum wind speed threshold was used because during clear nights with calm winds, it is possible for the air temperature, measured by a ventilated thermistor, to be underestimated by as much as 0.5°C (World Meteorological Organization 2010). The precipitation criterion was implemented to exclude heatbursts, sudden small-scale increases in temperature associated with decaying convective storms (McPherson et al. 2011). The latter two criteria were designed to capture periods of rapid warming and exclude events associated with synoptic-scale warming effects. Each threshold was tuned using manual analysis on individual cases of warming and nonwarming.

To contrast and compare conditions associated with warming events with conditions associated with no warming, it was useful to define control periods. As in the analysis of the cold front–associated warming events, all control periods were found within 24 h after a recorded cold-frontal passage time. These periods had to satisfy the same solar radiation, wind direction, and precipitation criteria stated above. Control periods, however, did not exhibit the

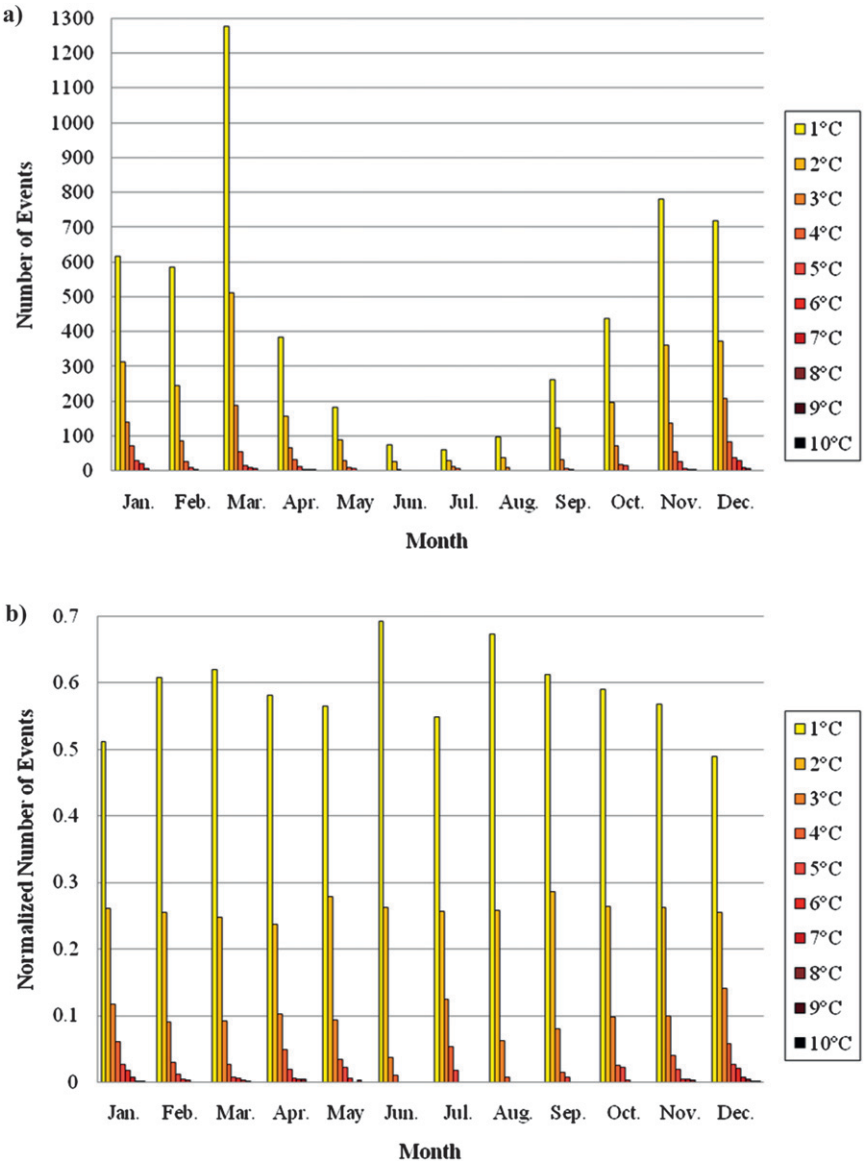

FIG. 7. (a) Total and (b) normalized number of warming events categorized by month and magnitude of warming. Bars for normalized events add up to 1 for each month.

10-min temperature increase of 1°C or larger. In other words, the control periods were nocturnal periods after a cold-frontal passage that did not contain warming events.

d. Additional terminology

We define several variables to help characterize environmental conditions prior to, during, and following warming events. These definitions should be borne in mind when considering the results presented in section 3.

As will be seen, it was common for several warming events to occur at a single station during the night. It is thus convenient to define a station night with warming (SNWW) as a night at a single station on which at least one warming event occurred. An example of an SNWW with multiple warming events is shown in Fig. 2.

The initial wind speed is defined as the average wind speed during the hour preceding the start of a warming event. For the control periods, the initial wind speed is defined as the average wind speed during the hour preceding the start of the control period. The warming-phase wind speed is the average wind speed during the warming phase of a warming event. The change in wind speed is the difference between the initial wind speed and warming-phase wind speed. In the case of a control period, the change in wind speed is defined as the difference between the initial wind speed and the wind

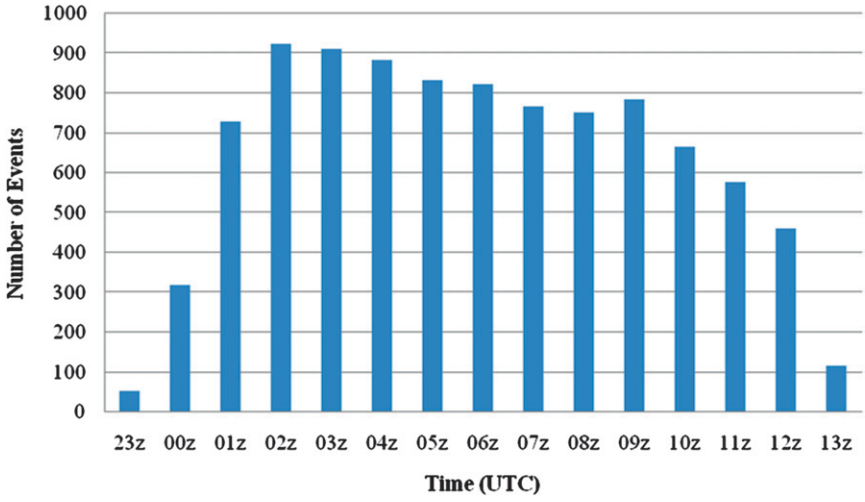

FIG. 8. Total number of warming events categorized by hour.

speed averaged over the control period. Positive values of change in wind speed indicate that the wind speed increased with time.

The temperature inversion strength is the difference in air temperature at 9 and 1.5 m AGL. Positive values indicate a temperature increase with height. The initial temperature inversion strength is the average temperature inversion strength during the hour preceding the start of a warming event, or, in the case of a control period, the average temperature inversion strength for the hour preceding the control period. The final temperature inversion strength is the average temperature inversion strength during the hour after the warming phase of a warming event or during the hour after a control period. Last, the change in temperature inversion strength is the difference between the final and initial temperature inversion strengths. Negative values indicate that the inversion weakened with time. As should be clear from these definitions, our focus is on low-level inversion strength. No attempt is made to characterize the thermal structure of the boundary layer above 9 m AGL.

3. Results

a. Overview of nocturnal warming events associated with cold fronts

During the 6-yr study period, there were a total of 9596 warming events and 6604 station nights with warming associated with 365 cold-frontal passages in Oklahoma. This corresponds to an average of 14.4 warming events and 9.9 SNWW per year for each Mesonet station. The difference between the total number of warming events and the total number of SNWW was attributed to the occurrence of multiple warming events at a single station during a single cold-frontal passage as illustrated in Fig. 2. Of all SNWW, approximately 29% contained multiple warming events.

The histogram of the magnitude of temperature increase with each warming event shows that a majority of the events were weak with 57.1% having increases less than 2°C (Fig. 3a). Only 3.1% of the warming events were characterized by significant warming with temperature increases exceeding 5°C. In terms of peak temperature increase, the top three warming events are 10.2°C at Clayton on 31 December 2008, 9.8°C at Inola on 4 January 2006, and 9.3°C at Wister also on 31 December 2008. All three locations are in eastern Oklahoma. A histogram of the duration of the warming events (Fig. 3b) indicates that although events could last as long as several hours, just over one-third (37.3%) were of short duration (<50 min), and the number of events lasting more than 50 min decreased roughly exponentially with increasing duration.

One of the main findings of our study was the surprisingly high frequency with which nocturnal warming events occurred. Of the 365 total cold fronts analyzed in this study, 91.5% (334 fronts) produced at least one warming event at a Mesonet station. Moreover, many of the 31 fronts that did not produce warming did not pass the detection criteria described in section 2c because they were associated with precipitation or did not pass through the entire state. For events that produced at least 2°C of warming, 78.9% (288 fronts) of the analyzed cold fronts produced at least one warming event. Overall, nocturnal warming events with cold-frontal passages were found to be weak and of short duration, but occurred with most cold fronts.

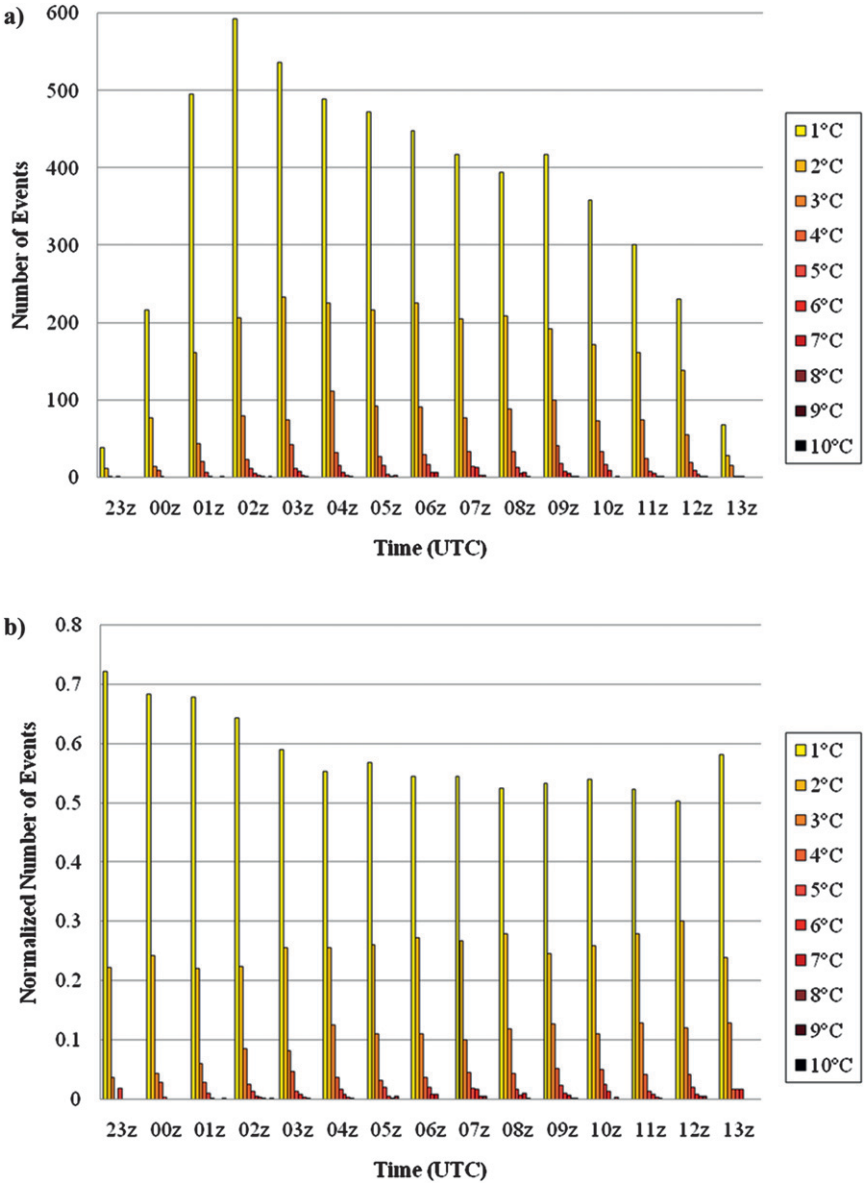

FIG. 9. As in Fig. 7, but categorized by hour rather than month.

The spatial pattern of warming as obtained from the objective analysis procedure described in section 3c and the temporal behavior of several variables were studied for selected cases. Figure 4 shows the peak 10-min temperature increase for the six events with the largest statewide number of SNWW. The warming pattern was generally structured in a narrow swath along the cold front. The higher-magnitude warming was localized to the position of the cold front, whereas the weaker warming events were more isolated and scattered away from the front. Meteograms of three of the strong warming events shown in Figs. 4a,c,e are displayed in Figs. 5a–c. For the purpose of comparison, a nocturnal cold-frontal passage with no associated warming (i.e., during a control period) is shown in Fig. 5d. One immediately sees pronounced differences in the temperature traces for the warming events and the control example. One may also note a rapid increase in pressure in the control example (which was typical of other control examples). Pressure rises were also found in these (and many other) warming events; these rises were generally much less pronounced than in the control cases, however. The conditions associated with the warming events were generally similar to those observed in previous studies (e.g., Doswell and Haugland 2007). Specifically, in the hours before warming occurred, wind speeds and gusts

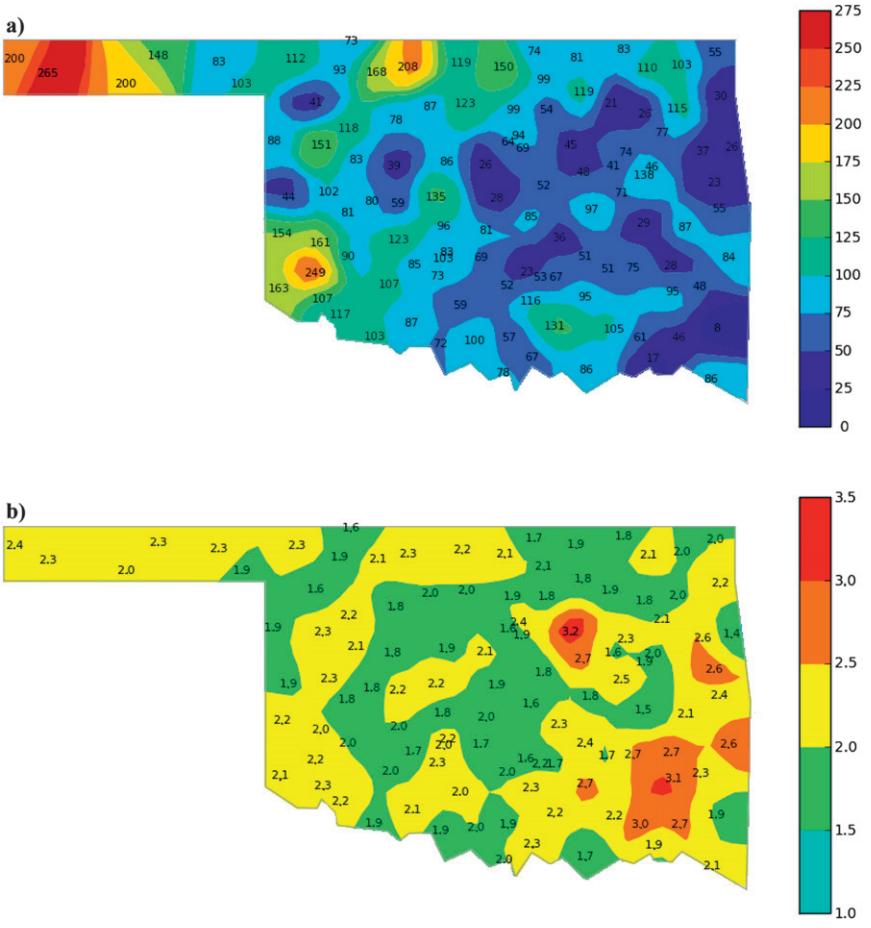

FIG. 10. Geographical distribution of (a) total number of warming events and (b) average magnitude of warming (°C).

were generally light (<~3 m s^{-1}) and temperatures typically dropped by ~2°C h^{-1}. However, we note that at one station (Bixby; Fig. 5c) prefrontal temperatures did not drop rapidly because conditions were close to saturated. This event also illustrates how a warming event can cause temperatures to increase above freezing, thus having potential implications for snowmelt and subsequent refreezing. The onset of all these warming events was characterized by a sudden surge in winds as the cold front passed through. Analyses in the next sections help to evaluate whether these observations are specific to these rather extreme cases or apply more generally.

b. *Temporal characteristics of warming events*

The warming events and SNWW were grouped by month as shown in Fig. 6a. Winter months had the most warming events (37.9%), and summer had the fewest (3.8%). Curiously, the month of March had the highest occurrence of warming events and SNWW; this month accounted for 21.5% of events and 19.2% of SNWW. December had the second highest occurrence of warming events (15.3%). June (followed by July and August) had the fewest occurrences of warming events (1.1%) and SNWW (1.5%). With the exception of March, the number of warming events and SNWW decreased from January to June and then increased until December. March, November, December, and January had the largest differences between warming events and SNWW; this implies that multiple warming events at a single station during a single cold-frontal passage occurred more frequently during these months. The summer months had the smallest differences.

It was instructive to also consider the number of monthly cold-frontal passages (Fig. 6b). The number of cold fronts ranged from 15 in July to 42 in March. Although there is clearly an association between the occurrences of warming events (blue bars in Fig. 6a) and the number of cold fronts (blue bars in Fig. 6b), the number of fronts did not solely dictate the number of

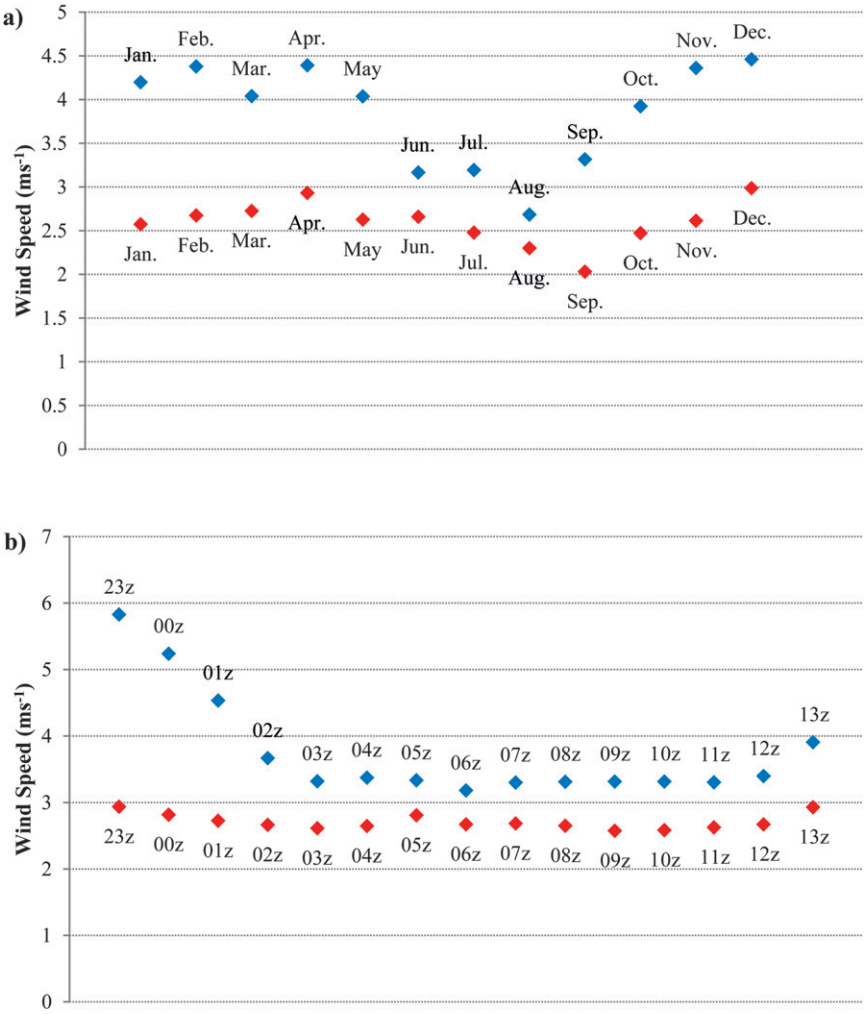

FIG. 11. Average initial wind speed at 10 m AGL for warming events (red) and control periods (blue) vs (a) month and (b) hour.

warming events that occurred. Indeed, the number of warming events normalized by the number of monthly cold-frontal passages (red bars in Fig. 6b) also exhibits a strong sensitivity to season and month. If the number of cold-frontal passages was the sole variable that affected the number of warming events that occurred, all months would have had very similar numbers of warming events per cold front. Evidently, the cool-season months yielded conditions that were more favorable for warming events to occur.

The occurrence of multiple warming events at a station during a single cold-frontal passage was a factor in the significant difference between the number of events occurring in summer and winter. Multiple warming events occurred most during the winter and least during the summer. Another reason why the summer months had the fewest warming events was because, in general, a larger percentage of cold fronts was associated with precipitation during this season. The precipitation criterion, therefore, would not have been fulfilled as frequently as it was in the winter. The change in the length of night also affected the seasonal variation of the occurrence of warming events. In the winter months, there was more time for warming events to occur since the nights were longer; the criterion that solar radiation had to be less than or equal to 5 W m^{-2} was fulfilled for more time in the winter than in the summer.

The number of warming events per month is further stratified by the magnitude of the warming (Fig. 7a). Although March had the most 1°C warming events, December had the largest number of strong warming events (i.e., warming $\geq$ 3°C), with 22.8% of all strong events. March came in second with 16.7%. With only 0.3% of all strong events, June had the fewest strong

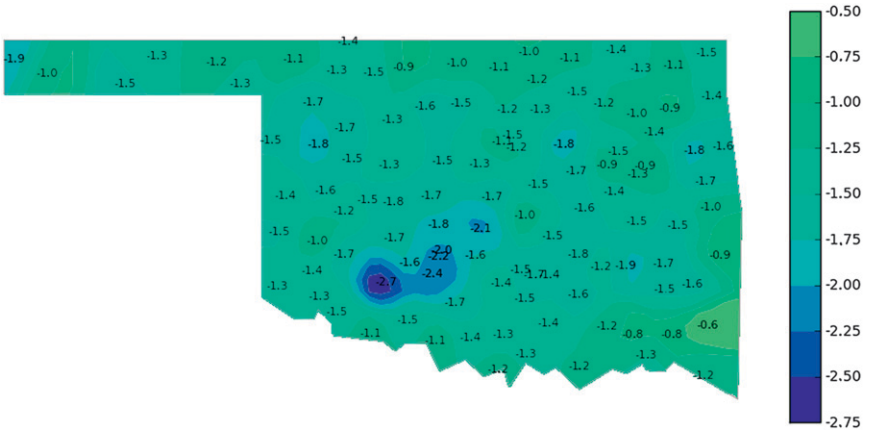

FIG. 12. Geographical distribution of the perturbation of average initial 10-m wind speed (m s^{-1}). Perturbation is the average initial wind speed for warming events minus that for control periods.

warming events. Next, we normalized the number of events in each warming magnitude category by the total number of warming events for each month (Fig. 7b). This analysis indicates that December and then January had the largest proportions of strong warming events with 25.7% and 22.8%, respectively, whereas June and August had the smallest proportions with 4.7% and 6.9%, respectively. In summary, the cool-season months that had the highest frequencies of warming events also had the largest proportion of the more significant events.

Next, we evaluated the hourly distribution of warming-event frequencies and magnitudes. Warming events occurred most infrequently at 2300 and 1300 UTC (Fig. 8). From 2300 UTC, the number of events increased until 0200 UTC at which time the maximum occurred. A gradual decrease took place thereafter until 1200 UTC. The low numbers of warming events during the beginning and end of the night can be partially explained by the variation of sunrise and sunset times during the year. The hourly frequency of warming events is further stratified by the magnitude of warming in Fig. 9a. The number of warming events in each magnitude class generally increased from 2300 until 0200–0300 UTC and then decreased throughout the rest of the night. However, the largest number of strong warming events (i.e., warming $\geq$ 3°C) occurred at 0900 UTC; 10.5% of all strong events were accounted for at this time. When we normalized the frequency of magnitude classes by the total number of events that occurred each hour in Fig. 9b, we could see that the largest proportion of weak warming events (1°C) occurred during the first hour of the night and then the proportion decreased thereafter. Moreover, we can see that the magnitude of the warming events is correlated with the increasing hour in the night; that is, stronger events tended to occur later in the night. The physical interpretation is that the weaker inversions that set up early in the night were more susceptible to being mixed out and a weaker warming event resulted because of the shallow depth of the early nocturnal inversion. Strong warming events occurred later in the night when the nocturnal inversion was deeper and more fully developed. Since the surface air temperature cooled more with these stronger inversions, the warming perturbation was stronger.

c. *Spatial characteristics of warming events*

To assess how warming events and the conditions associated with them varied spatially across Oklahoma, Mesonet data were objectively analyzed using a Barnes scheme (Barnes 1964; Koch et al. 1983). The Barnes objective analysis uses an exponential weighting function with a user-specified *e*-folding distance to interpolate irregularly distributed observations to a set of regularly spaced Cartesian grid points. We applied the Barnes scheme to the Mesonet data with an *e*-folding distance of 21 km. Although there is much site-specific variability in the frequency of warming events, a spatial analysis (Fig. 10a) reveals a pronounced east–west gradient in warming-event frequency. Boise City in the western panhandle had the most events (265) while Mount Herman in the southeast had the fewest (8). Although the number of cold-frontal passages decreased from the panhandle to the southeast (not shown), the difference in the number of fronts between the panhandle and southeast climate divisions (43) was much too small to explain why Boise City had at least 200 more warming events than Mount Herman.

Interestingly, a spatial analysis of the average magnitude of warming events showed that the largest-magnitude events tended to occur in the eastern part of the state

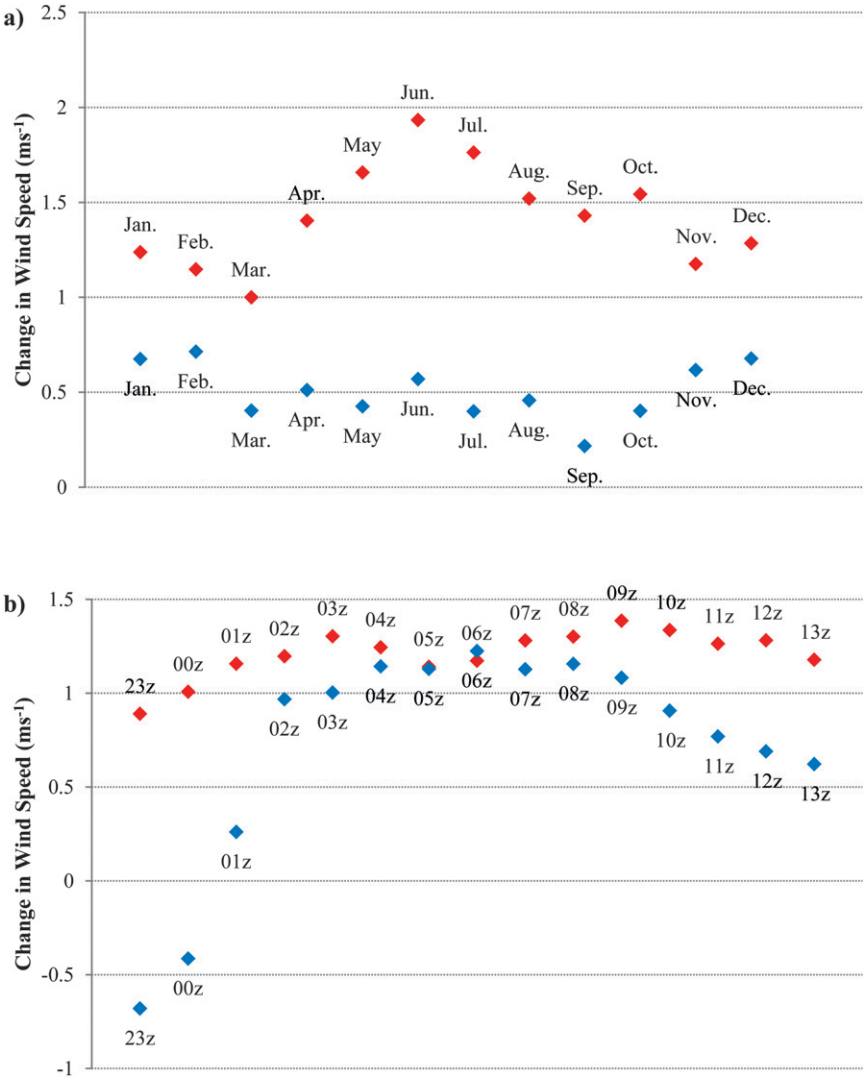

FIG. 13. As in Fig. 11, but for average change in wind speed.

(Fig. 10b). That is, the gradient of the magnitude was generally opposite that of the gradient of the event frequency. The eastern stations Oilton, Clayton, and Antlers had the highest values with averages of at least 3°C of warming. If we were to define a metric for total (integrated) station warming based on the frequency of warming events and the average magnitude of warming events, it is apparent that, in the west, the much higher frequencies would more than compensate for the somewhat lower-average warming. As a result, the integrated warming would be much greater in western Oklahoma.

Additional analysis of these results will be required to resolve the gradients and the site-specific maxima. In general, Oklahoma's terrain is gently sloping with height increasing to the west, but the eastern part of the state has much more complex topography. Much of the eastern part of the state is forested whereas the west is characterized by prairie vegetation and farmland. It is plausible that the combination of a forested land surface along with complex topography created shielding conditions that promoted enhanced surface cooling in advance of the mixing. An explanation for the site-specific maxima in warming frequencies and magnitudes, including the possible role of the surrounding terrain and vegetation, is a topic for future research.

d. Conditions associated with warming events

Since the initial wind speed is an important factor in the production and maintenance of a nocturnal temperature inversion, it would, therefore, also likely be an important factor in the occurrence of warming events. Light–calm winds inhibit the mixing of air from aloft and help

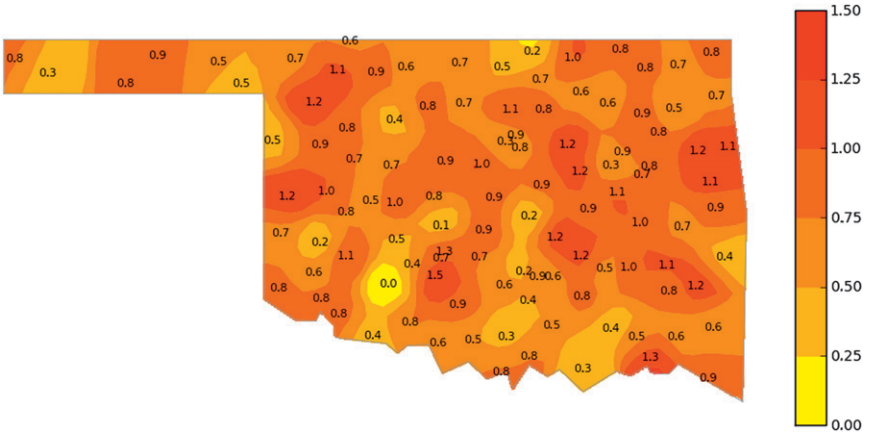

FIG. 14. As in Fig. 12, but for the average change in 10-m wind speed (m s^{-1}).

enhance cooling at the surface, thus strengthening the nocturnal inversion (Wallace and Hobbs 2006). Figures 11 and 12 show the temporal (hourly and monthly) and geographical distribution of the average initial wind speed at 10 m AGL for the warming events and the control periods. The initial wind speed for the warming events was always lower than that for the control periods at the monthly (Fig. 11a) and hourly scale (Fig. 11b). In fact, an average initial wind speed threshold of ~3 m s^{-1} segregates the warming events and control periods quite well. Presumably, the lower wind speeds facilitate the development of a nocturnal temperature inversion. It is also noted that the months and hours with the greatest frequency of warming events have the largest discrepancies in initial wind speeds between the control period and event databases. The spatial distribution of the perturbation of average initial wind speed (average initial wind speed for warming events minus that for control periods) depicted in Fig. 12 shows that, relative to control periods, warming events were preceded by smaller wind speeds. This perturbation is roughly constant across the state.

Next, we examined the temporal and geographic distribution of the change in 10-m wind speed for warming events and control periods. The average change in wind speed was higher for warming events than for control periods for every month and hour, with the exception of 0600 UTC (Fig. 13). This result suggests that the turbulent mixing of air from aloft down to the surface, induced by the cold-frontal passage, was important in the production of warming. The distribution of the perturbation of the average change in wind speed (average change in wind speed for warming events minus that for control periods) shown in Fig. 14 shows that larger changes were associated with the warming events. No apparent trend was evident in this perturbation.

We have hypothesized that an initial, strong temperature inversion is an important factor in the production of warming events in our dataset, perhaps with stronger initial inversions resulting in stronger warming events. Figure 15a shows how the average initial temperature inversion strength (as determined by the difference between 9- and 1.5-m air temperature) varied by month for the warming events and the control periods. The average initial inversion strength for the warming events was always higher than that for the control periods for each month, indicating the importance of this factor. Figure 15b shows a correlation between the average initial temperature inversion strength for the warming events and the control periods. This is likely because the process of inversion formation is similar for both the pre-warming environment and the control environment. As described by Geiger et al. (1995), a surface-based temperature inversion rapidly develops after sunset and then becomes relatively stable. During the first 1–2 h after sunset, the vertical temperature gradient of the inversion is at its strongest. One reason why the most warming events occurred at ~0200 UTC could be because temperature inversions were near their peak strengths at that time and were so shallow that they were particularly vulnerable to higher-momentum winds associated with the cold front that can mix air from aloft down to the surface. After ~0200 UTC, as the inversion grew in depth—thus producing a slightly weaker temperature gradient at the surface—a vertical exchange of air parcels during a mixing event would be somewhat less effective in raising the temperature at the surface.

Figure 16 shows how the perturbation of the average initial temperature inversion strength (average initial temperature inversion strength for warming events minus that for control periods) varied across Oklahoma. At every station, the average initial temperature inversion

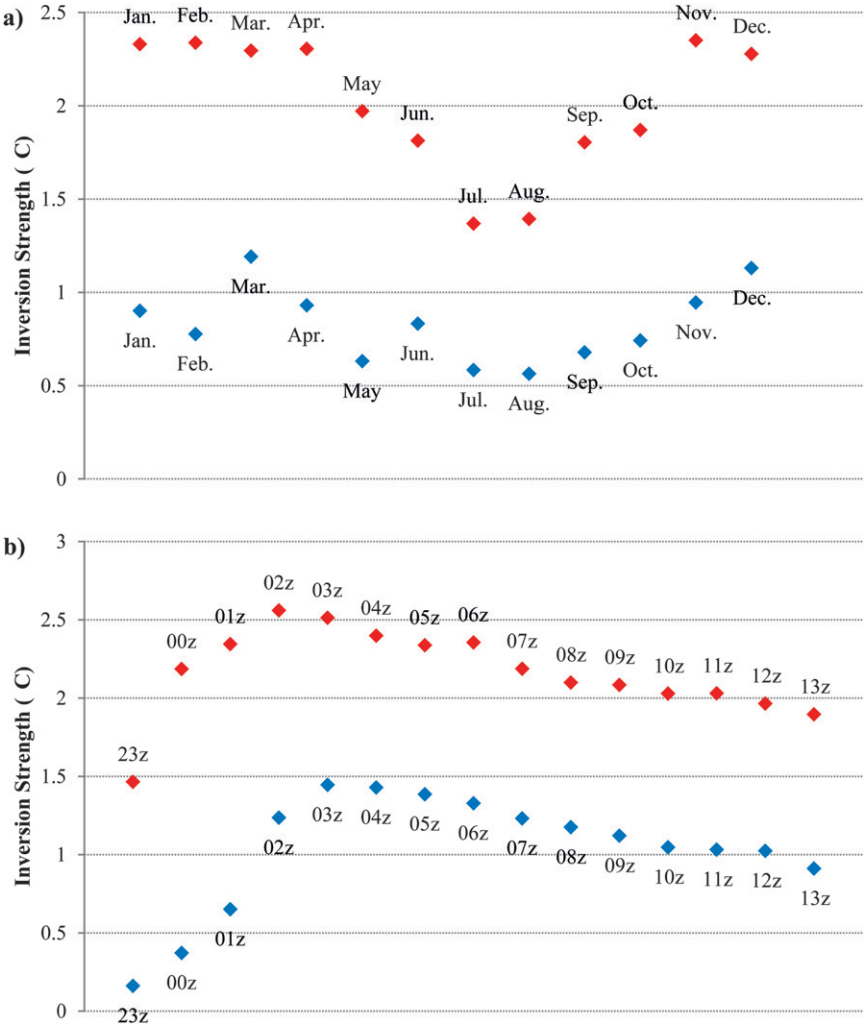

FIG. 15. Average initial temperature inversion strength for warming events (red) and control periods (blue) vs (a) month and (b) hour.

was stronger for warming events than for control periods. The trend was for this perturbation to increase toward the east.

The temporal distribution of the average change in temperature inversion strength for warming events and control periods is presented in Fig. 17. The temperature inversion always weakened more with the warming events than with the control periods. This result, combined with the wind speed analysis, strongly suggests that the mechanism that produced warming was the breakdown of the nocturnal inversion by vertical mixing of relatively warm air down to the surface. The mixing was facilitated by the strong winds attending the cold-frontal passages. There did not appear to be a significant geographical distribution in the average change in temperature inversion strength for the warming events or the control periods (not shown).

Nocturnal warming events associated with cold-frontal passages have been shown to be associated with initially weak surface wind speeds and strong temperature inversion strengths. Of all the observed 9596 warming events in this study, 84.4% occurred when initial wind speeds were less than 4 m s^{-1} and 62.9% occurred when initial speeds were less than 3 m s^{-1}. At least 99% of the observed warming events took place when a temperature inversion was present at the surface. By the end of the warming phase, the wind speed had increased in 87.4% of the cases (see definition of change in wind speed in section 2d). In 87.7% of the warming events, the temperature inversion had weakened (see definition of change in inversion strength in section 2d). For more significant events that produced at least 2°C of warming, 93.7% of the warming events were associated with increased surface wind speeds, and 93.3% had weaker

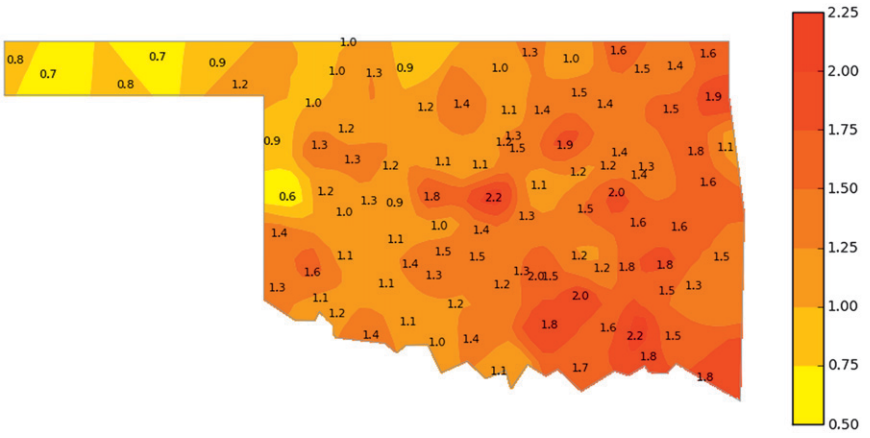

FIG. 16. As in Fig. 12, but for the average initial temperature inversion strength (°C).

resulting inversion strengths. Given these statistics on the onset of warming events, it would seem plausible that the initial wind speed and temperature inversion strength should be correlated with the magnitude of surface warming. We computed Pearson linear correlation coefficients of the magnitude of warming with the following variables: initial wind speed, initial temperature inversion strength, change in wind speed, and change in inversion strength. However, all of the correlations were generally quite weak ($\rho < |0.5|$). It is possible that some combinations of multiple conditions (e.g., weak initial wind speed and strong inversion strength) would be better correlated with the magnitude of warming. Another explanation for the weak correlations is that the statistical analysis did not take into account additional factors that were shown to be important such as the hourly and monthly changes or geographic distribution of conditions across the state. In any case, an account of the factors controlling the magnitude of the warming events might benefit from augmenting a statistical characterization with results from a numerical modeling approach.

4. Summary

A climatological analysis of nocturnal warming events associated with cold-frontal passages over Oklahoma was conducted with 6 yr of Oklahoma Mesonet data. Nocturnal warming events occurred surprisingly frequently, with 91.5% of cold fronts producing at least one warming event across the state. Although the majority of these events were relatively weak (~1°C warming), some rare events produced up to ~10°C of warming. The winter months accounted for the most events (37.9%), which was still the case when we normalized the event frequency by the number of cold-frontal passages. The number of warming events increased from 2300 until 0200–0300 UTC and then decreased throughout the rest of the night. However, the largest number of strong warming events (i.e., warming ≥ 3°C) occurred much later in the night at 0900 UTC; 10.5% of all strong events were accounted for at this time. The frequency of warming events generally decreased from west to east, which was opposite the gradient of the magnitude of warming events.

Of all the 9596 warming events identified, 84.4% occurred when initial wind speeds were less than 4 m s^{-1}, and more than 99% took place when a temperature inversion was present at the surface. By the end of the warming phase, the wind speed had increased in 87.4% of the cases. In 87.7% of the warming events, the temperature inversion had weakened. These percentages increased to >93% with warming events that increased the surface temperature by >2°C. Our results are consistent with previous studies that indicate that warming was due to the mixing of warmer air aloft down to the ground by the strong and gusty winds accompanying cold-frontal passages.

Several features revealed by the climatological analysis highlight questions for future research. For instance, why would March stand out as the month with the most warming events (and the most warming events per cold front)? What processes affect the eastward increase in the intensity of the warming events? What processes affect the very pronounced westward increase in the number of warming events? Although warming events were usually associated with weak initial wind speeds, why was there a low correlation between initial wind speed and magnitude of warming? Similarly, although warming events were more associated with strong initial temperature inversions than nonwarming events in the control period, why was there a low correlation between initial inversion strength and magnitude of warming? Detailed observational case studies and high-resolution

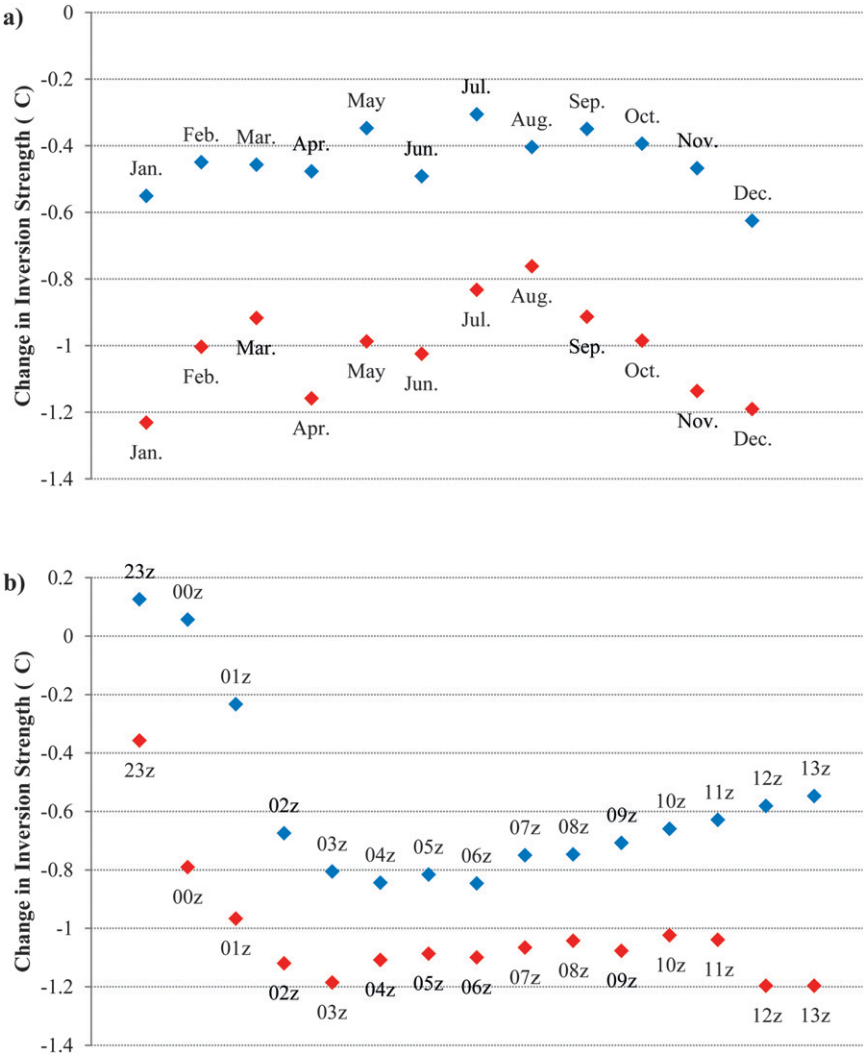

FIG. 17. As in Fig. 15, but for the average change in the temperature inversion strength.

numerical model simulations might shed some light on these questions.

Acknowledgments. Oklahoma Mesonet data are provided courtesy of the Oklahoma Mesonet, a cooperative venture between the University of Oklahoma (OU) and Oklahoma State University supported by Oklahoma taxpayers. We are also grateful to Fred Carr (OU School of Meteorology), Chris Fiebrich (Oklahoma Climatological Survey), and Mike Hansen (Campbell Scientific) for their comments and advice.

REFERENCES

Barnes, S. L., 1964: A technique for maximizing details in numerical weather map analysis. *J. Appl. Meteor.,* **3,** 396–409.

Beringer, J., and N. J. Tapper, 2000: The influence of subtropical cold fronts on the surface energy balance of a semi-arid station. *J. Arid Environ.,* **44,** 437–450.

Brock, F. V., K. C. Crawford, R. L. Elliot, G. W. Cuperus, S. J. Stadler, H. L. Johnson, and M. D. Eilts, 1995: The Oklahoma Mesonet: A technical overview. *J. Atmos. Oceanic Technol.,* **12,** 5–19.

Clarke, R. H., R. K. Smith, and D. G. Reid, 1981: The morning glory of the Gulf of Carpentaria: An atmospheric undular bore. *Mon. Wea. Rev.,* **109,** 1726–1750.

Colorado State University, 2009: NWS DIFAX weather map archive. [Available online at http://archive.atmos.colostate.edu/.]

Doswell, C. A., and M. J. Haugland, 2007: A comparison of two cold fronts—Effects of the planetary boundary layer on the mesoscale. *Electron. J. Severe Storms Meteor.,* **2,** 1–12.

Fiebrich, C. A., and K. C. Crawford, 2001: The impact of unique meteorological phenomena detected by the Oklahoma Mesonet and ARS Micronet on automated quality control. *Bull. Amer. Meteor. Soc.,* **82,** 2173–2187.

Geiger, R., R. H. Aron, and P. E. Todhunter, 1995: *The Climate near the Ground*. 5th ed. Vieweg and Sohn, 528 pp.

Haugland, M. J., 2006: The Crosstimber Micronet: An automated microscale surface observation network. Preprints, *10th Symp. on Integrated Observing and Assimilation Systems for the Atmosphere, Oceans, and Land Surface,* Atlanta, GA, Amer. Meteor. Soc., 4.1. [Available online at http://ams.confex.com/ams/pdfpapers/103127.pdf.]

Koch, S. E., M. desJardins, and P. J. Kocin, 1983: An interactive Barnes objective map analysis scheme for use with satellite and conventional data. *J. Climate Appl. Meteor.,* **22,** 1487–1503.

McPherson, R. A., and Coauthors, 2007: Statewide monitoring of the mesoscale environment: A technical update on the Oklahoma Mesonet. *J. Atmos. Oceanic Technol.,* **24,** 301–321.

——, J. D. Lane, K. C. Crawford, and W. G. McPherson Jr., 2011: A climatological analysis of heatbursts in Oklahoma (1994–2009). *Int. J. Climatol.,* **31,** 531–544.

National Centers for Environmental Prediction, 2009: Daily weather maps. [Available online at http://www.hpc.ncep.noaa.gov/dailywxmap/.]

National Climatic Data Center, 2009: U.S. climate divisions boundary files (GIS). [Available online at http://lwf.ncdc.noaa.gov/oa/climate/surfaceinventories.html#gis.]

Reeder, M. J., R. K. Smith, R. Deslandes, N. J. Tapper, and G. A. Mills, 2000: Subtropical fronts observed during the 1996 Central Australian Fronts Experiment. *Aust. Meteor. Mag.,* **49,** 181–200.

Sanders, F., and E. Kessler, 1999: Frontal analysis in the light of abrupt temperature changes in a shallow valley. *Mon. Wea. Rev.,* **127,** 1125–1133.

Shafer, M. A., T. Hughes, and J. D. Carlson, 1993: The Oklahoma Mesonet: Site selection and layout. Preprints, *Eighth Symp. on Meteorological Observations and Instrumentation,* Anaheim, CA, Amer. Meteor. Soc., 231–236.

——, C. A. Fiebrich, D. S. Arndt, S. E. Fredrickson, and T. W. Hughes, 2000: Quality assurance procedures in the Oklahoma Mesonet. *J. Atmos. Oceanic Technol.,* **17,** 474–494.

Shapiro, A., P. M. Klein, S. C. Arms, D. Bodine, and M. Carney, 2009: The Lake Thunderbird Micronet Project. *Bull. Amer. Meteor. Soc.,* **90,** 811–823.

Smith, R. K., M. J. Reeder, N. J. Tapper, and D. R. Christie, 1995: Central Australian cold fronts. *Mon. Wea. Rev.,* **123,** 16–38.

Unisys Weather, 2009: Image and map archive. [Available online at http://weather.unisys.com/archive/index.html.]

Wallace, J. M., and P. V. Hobbs, 2006: *Atmospheric Science: An Introductory Survey*. Academic Press, 483 pp.

White, L. D., 2009: Sudden nocturnal warming events in Mississippi. *J. Appl. Meteor. Climatol.,* **48,** 758–775.

World Meteorological Organization, 2010: WMO guide to meteorological instruments and methods of observation. [Available online at http://www.wmo.int/pages/prog/www/IMOP/publications/CIMO-Guide/CIMO_Guide-7th_Edition-2008.html.]